Journal of Materials Chemistry B

PAPER

Cite this: J. Mater. Chem. B, 2015, 3, 8823

Nerve conduits constructed by electrospun P(LLA-CL) nanofibers and PLLA nanofiber yarns

Dawei Li,[ab] Xin Pan,[b] Binbin Sun,[b] Tong Wu,[b] Weiming Chen,[b] Chen Huang,[a] Qinfei Ke,*[ac] Hany A. El-Hamshary,[de] Salem S. Al-Deyab[d] and Xiumei Mo*[ab]

Received 14th July 2015,
Accepted 8th October 2015

DOI: 10.1039/c5tb01402f

www.rsc.org/MaterialsB

Injuries of the peripheral nerve occur commonly in various people of different ages and backgrounds. Generally, surgical repairing, such as suturing the transected nerve stumps and transplanting an autologous nerve graft, is the only choice. However, tissue engineering provides an alternative strategy for regeneration of neural context. Functional nerve conduits with three dimensional (3D) support and guidance structure are badly in need. Herein, a uniform PLLA nanofiber yarn constructed by unidirectionally aligned nanofibers was fabricated *via* a dual spinneret system, which was subsequently incorporated into a hollow poly(L-lactide-*co*-caprolactone) (P(LLA-CL)) tube to form a nerve conduit with inner aligned texture. The biocompatibility of the poly(L-lactic acid) (PLLA) yarn was assessed by *in vitro* experiments. Schwann cells (SCs) presented a better proliferation rate and spread morphology of the PLLA yarn than that of PLLA film. Confocal images indicated that the axon spreads along the length of the yarn. SCs were also cultured in the conduit. The data indicated that SCs proliferated well in the conduit and distributed dispersedly throughout the entire lumen. These results demonstrated the potential of the PLLA nanofiber yarn conduit in nerve regeneration.

1. Introduction

Peripheral nerve injury is a common global problem occurring to people of different backgrounds, which often leads to the loss of sensory and motor functions. Various methods were invented to repair the nerve injury. Surgically, short nerve lesion can be appropriately repaired by end to end coaptation. However, for the long distance nerve defection, end to end anastomosis is no longer an option as it causes detrimental tension along the nerves and retards healing.[1] In these cases, a graft is needed to bridge the nerve gap and provide better regenerative outcomes. Currently, autologous nerve grafts are considered as the "gold standard" for gap injuries greater than 5–10 mm.[2] However, some drawbacks restrict its application, such as the limited donor resource, sacrifice of the donor, extra incision, and possible size mismatch. Customized grafts for specific nerve injuries are desired for better cure with little side effect and additional sacrifice.

The progress of tissue engineering scaffolds provides a promising alternative for nerve repair. Nerve conduits can act as a bridge between adjacent ends, providing directional guidance and biological support during nerve regeneration. To better adjust the interaction of cells, tissue, and the conduit, scaffolds with nanoscale topology are extensively introduced in the manufacture of nerve scaffolds. Diverse fabrication methods have been used to prepare nanostructured scaffolds, such as phase separation,[3,4] self-assembly,[5] as well as electrospinning.[6–8] The most commonly used designs include hollow tubes (Fig. 1(a)), multiple channel conduits (Fig. 1(b)), tubes filled with internal matrices with longitudinal oriented channels or pores (Fig. 1(c)),[9–12] as well as lumen filled with aligned polymer fibers as longitudinal guidance (Fig. 1(d) and (e)).[8,13–21]

Electrospinning is mostly reported due to its easy handling ability, cost efficiency, quality controllability, and availability for various natural and synthetic materials. Electrospun nanofiber scaffolds can mimic the basic nanoscale structure of the natural extracellular matrix. Parallel fibers have demonstrated the ability to guide the spreading and migration of Schwann cells (SCs).[8,22–24] Additionally, aligned fibers may induce the differentiation and maturation of neural stem cells and SCs.[25,26] Dorsal root ganglia (DRG) cultured on the parallel nanofiber tend to generate long and unidirectionally ordered neurites. The predetermined aligned nanofibers could cause SC alignment and subsequent neurite extension *in vitro*. Studies also have shown that the unidirectional electrospun nanofiber, but not

[a] Engineering Research Center of Technical Textiles, College of Textiles, Donghua University, Shanghai 201620, China. E-mail: xmm@dhu.edu.cn, kqf@dhu.edu.cn
[b] State Key Lab for Modification of Chemical Fibers & Polymer Materials, College of Chemistry, Chemical Engineering and Biotechnology, Donghua University, Shanghai, 201620, China
[c] Shanghai Normal University, Shanghai, 200234, China
[d] Department of Chemistry, College of Science, King Saud University, Riyadh, Kingdom of Saudi Arabia
[e] Department of Chemistry, Faculty of Science, Tanta University, Tanta, Egypt

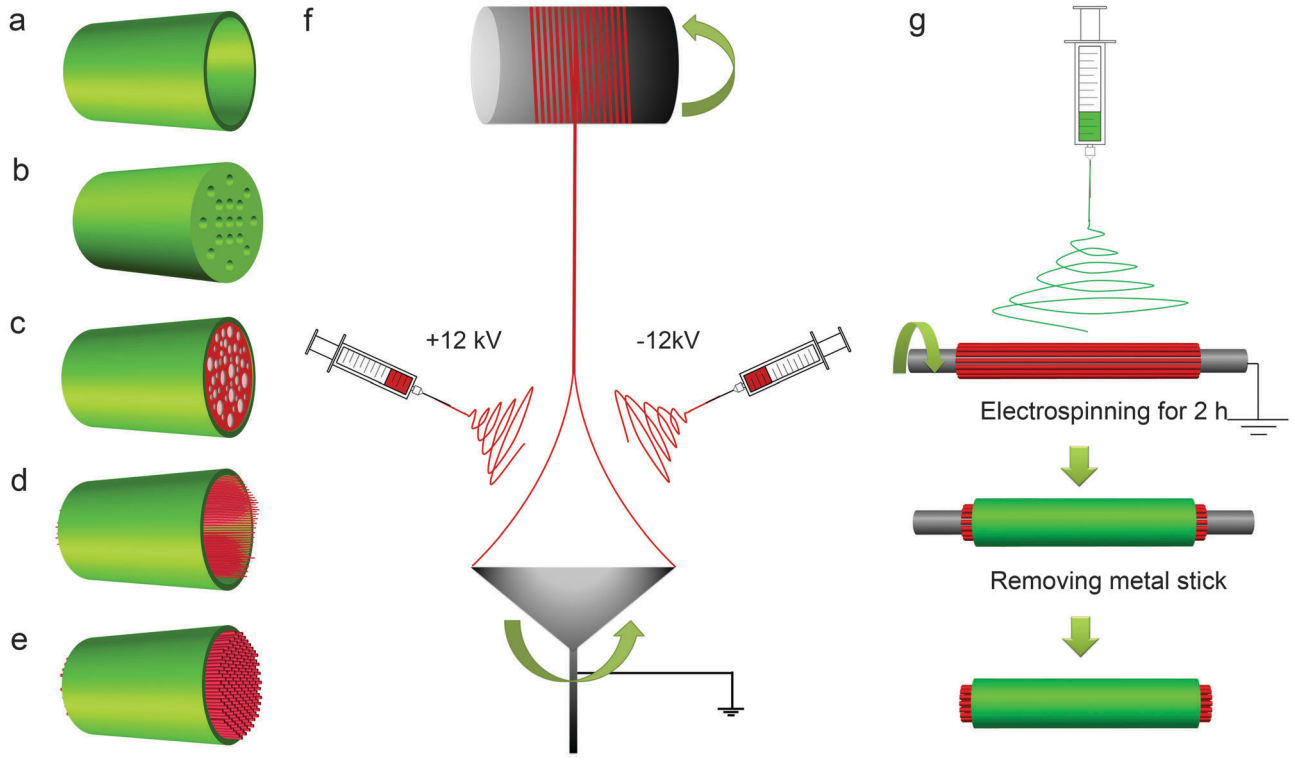

Fig. 1 Schematic of various conduits: (a) hollow lumen conduit, (b) multichannel conduit, (c) sponge-containing conduit, (d) fiber-containing conduit, and (e) nanofiber yarn-containing conduit. (f) The mechanism of nanofiber yarn fabrication. (g) Schematic of incorporating the nanofiber yarn into the conduit.

the randomly oriented nanofiber, could guide nerve regeneration across long nerve gaps.[19] However, the traditional electrospinning process is always used to manufacture 2D film with densely compacted structure which inhibited cell infiltration and immigration into the scaffold.[27] Andreas Kriebel *et al.* have tried the v-shaped collector to collect aligned nanofibers with 3D structure which was subsequently incorporated into the collagen matrix.[21] The guiding function of the parallel nanofiber was struck as axons also adhere to the surrounding hydrogel. Several types of nerve conduits have been designed to incorporate aligned electrospun nanofibers into the inside of the tube. The most commonly used method is to fabricate tubes with axially aligned nanofibers constructing the inner surface of the tube.[23,28,29] Jingwei Xie *et al.* fabricated double layered nerve conduits with the aligned PCL nanofiber as the inner surface while the random fiber served as the supporting wall.[23] *In vivo* results indicated that bilayer conduits could effectively improve nerve fiber sprouting and motor recovery. This approach facilitated cell spreading and migration but did not provide effective support for cell growth in the space of the lumen. Eric M. Jeffries *et al.* reported 3D multichannel nerve conduits incorporated with parallel electrospun fibers.[18] This guide had thin walls and high channel numbers to maximize the surface area and facilitate cell spreading and migration. However, the manufacturing process was labor intensive and varied by operators, which limited the effective conduit length and reproducibility. Another commonly used method is to insert a bundle of aligned nanofibers in the nerve guide.[15,17,19–21] Highly aligned nanofiber film was cut into thin strips and incorporated in a hollow nerve conduit by Young-tae Kim *et al.*[19] The presence of aligned nanofiber film could maximize the topographic directional cues for neurite outgrowth and SC migration in a 3D configuration. However, the width of the stripes may also lead to unevenness of tissue regeneration in the sectional direction. 3D scaffolds consisting of parallel fibers were fabricated *via* modulating the collector by Andreas Kriebel *et al.*[21] and Balendu S. Jha *et al.*[15] Both studies demonstrate that the parallel fibers could direct axonal regeneration and SC migration along a defined axis. Nevertheless, the scaffolds constructed by parallel fibers were quite soft and difficult to handle. Moreover the densely packed nanofibers may inhibit cell infiltration.[21,27]

In this study, a novel approach is introduced in manufacturing of long distance nerve conduits with aligned electrospun nanofibers as the filler and randomly electrospun nanofibers as the shell. Our method is based on the fabrication of nanofiber yarns by a dual spinneret electrospinning system. The yarn constructed by nanofibers inherits various features of nanofibers, but also possessed unique properties such as easy post-processing. Nanofiber yarns can be manufactured by textile and related methods into a fabric and other predetermined structures. Various techniques were introduced to fabricate nanofiber yarns. Ko *et al.* studied firstly an electrospun continuous nanoscale composite yarn with a complex setup with orientation, twisting, and take up components.[30] Smit *et al.* drawn the electrospun nanofiber web from the water bath and collected continuous yarns.[31] Teo *et al.* used the water vertex, which is

water flowing from the hole of a basin to generate a continuous nanoscale yarn.[32] A grounded tip was applied to induce the self-bundling nanofiber yarn by Wang *et al.*[33] Recently, the nanofiber yarn was fabricated by the oppositely charged dual nozzle system.[34–36] In which, the nanofiber yarn could be twisted and collected at the same time.

Herein, the PLLA nanofiber yarn was fabricated using the dual nozzle electrospinning system. The random nanofibers electrospun from P(LLA-CL) solution possess excellent mechanical properties for the nerve conduits and provide the conduit tear-resistant during the surgical procedure. Whereas the highly aligned nanofiber in the nanofiber yarn made of PLLA serves as the guidance for axon spreading and cell migration. Characterization of the PLLA nanofiber yarn and the nerve conduit was conducted, while SCs were cultured on the PLLA nanofiber yarn and in the nerve conduits to study the biological performance.

2. Materials and experiments

2.1 Materials

PLLA with an average molecular weight (M_w) of 500 kDa was purchased from Daigang Biomaterials Inc. (Jinan, China). P(LLA-CL) (M_w = 300 kDa, LA : CL = 50 : 50) was supplied by Nara Medical University, Japan. Hexafluoroisopropanol (HFIP) was obtained from Shanghai Darui Fine chemicals Co., Ltd (China). The Dulbecco's Modified Eagle's Medium (DMEM, Hyclone), fetal bovine serum (FBS, Gibico), trypsin (hyclone) and 3-(4,5-dimethylthiazol-2-yl)-2,5-diphenyltetrazoliumbromide (MTT, Sigma) was purchased from Yuanzhi Biotechnology Co., Ltd (Shanghai, China). 4′,6-Diamidino-2-phenylindole (DAPI) and Alexa Fluor® 568 phalloidin was supplied by Life Technologies Co., Ltd (USA).

2.2 Preparation of PLLA nanofiber yarns

0.75 g PLLA was dissolved in 10 mL of HFIP to generate 7.5% w/v PLLA solution. The nanofiber yarn was fabricated by a dual spinneret electrospinning system as described by Usman Ali *et al.*[36] As illustrated in Fig. 1(f), the setup consists of two spinnerets, a plastic funnel (diameter = 10 mm) with a conductive edge which was grounded, a yarn winder (diameter 8 mm), and two high voltage DC power supplies (Gamma High Voltage Research, USA). During electrospinning, the PLLA solution was taken in the two oppositely positioned syringes and squeezed out through the metal needles of 20 gauge. The flow rate of PLLA solution was set at 1.0 mL h^{-1}. Two needles were separately charged with positive (+12 kV) and negative (−12 kV) high voltages. Electrospun nanofibers from two nozzles were deposited on the rotary funnel and covered the funnel end with a nanofiber layer. A cone shaped nanofiber layer could form on the funnel edge by the initial inducing step. After drawing by the winder and twisting by the rotary funnel, a continuous nanofiber yarn was obtained. As a control, PLLA nanofiber film was prepared using a single electrospinning nozzle and collected on aluminum foil. The voltage, spinning rate, and collecting distance were set as +12 kV, 1.0 mL h^{-1}, and 15 cm, respectively.

2.3 Characterization

The surface of the nanofiber yarn was sputter-coated with gold and subsequently observed using a Digital Vacuum Scanning Electron Microscope (SEM, TM 3000, Hitachi, Japan) at the accelerating voltage of 15 kV. The diameter of fibers in the nanofiber yarn was measured by the SEM images using the image visualization software Image J (National Institutes of Health, USA). 100 fibers were randomly selected for each sample.

2.4 *In vitro* experiments

SCs were maintained and expanded in DMEM culture medium, incubated in a humidified atmosphere with 5% CO_2 at 37 °C. The culture medium was refreshed every other day. For *in vitro* biocompatibility assessment, the PLLA nanofiber yarn was wounded on a square glass slip (a side of 10 mm) till the entire surface was covered by the yarn. The PLLA film was cut into round pieces with a diameter of 15 mm. The samples were fixed in the 24-well culture plates by stainless steel rings with an inner diameter of 10 mm. Subsequently, the plates were sterilized by alcohol steam in a sealed desiccator for 48 h. Scaffolds in the plate were rinsed with phosphate-buffered saline solution (PBS) 3 times and washed with culture medium once.

2.5 Adhesion and proliferation of SCs

For the assessment of SC adhesion on the PLLA nanofiber yarn, a total number of 4×10^4 cells were seeded on the scaffolds in a 24-well plate to compare the cell adhesion PLLA nanofiber yarn and film with tissue culture plates (TCPs) as control. 40 min, 60 min, 120 min and 240 min after seeding, the culture medium was removed and the specimens were rinsed with PBS 3 times to remove the unattached and dead cells. Then, the amount of the attached cells was determined by standard MTT assay. Briefly, the specimens were incubated in 360 μL FBS-free DMEM culture medium and 40 μL 5 mg mL^{-1} MTT solution for 4 h. Thereafter, the culture media were pipetted out and 400 μL of dimethylsulfoxide (DMSO) was added. Afterwards, the plate was incubated in a shaker at 37 °C for 30 min. While the crystal was thoroughly dissolved, 100 μL of the solution was transferred to a 96-well plate and tested using a microtiter plate reader (Multiskan MK3, Thermo, USA), at the absorbance of 492 nm.

For the proliferation study, 1×10^4 cells were seeded on the scaffolds with TCP as control. The amount of cells on each specimen was determined by the standard MTT assay. 1, 3, and 7 days of post-seeding, the culture medium was removed and unattached cells were washed away with PBS three times, MTT assay was conducted as described above to determine the amount of viable cells on the scaffolds. For each group 6 specimens were tested.

2.6 Cell morphology observation

A total number of 1.0×10^4 cells were seeded on the nanofiber yarn and film in 24-well plates. After culturing for 1, 3, and 7 days,

cells cultured on the scaffolds were fixed by 4% paraformaldehyde for 2 h at 4 °C, dehydrated with gradient ethanol solution (30%, 50%, 70%, 90%, 95%, and 100%) and followed by freeze drying at −60 °C for 12 h. Afterwards, the samples were sputter coated with gold and observed by SEM at the accelerating voltage of 15 kV.

Confocal laser scanning microscopy (CLSM, Carl Zeiss, LSM 700, Germany) was used to visualize the morphology and distribution of cells on the scaffolds. After 1, 3, and 7 days of culture, the specimens with cells were rinsed twice with PBS and then fixed with 4% paraformaldehyde for 2 h at 4 °C. Subsequently, the cells on the scaffolds were permeabilized by 0.1% Triton X-100 (Sigma, USA) for 10 min. After rinsing 3 times with PBS, the cytoskeletons and nuclei of cells were stained with 25 μg mL^{-1} of rhodamine-conjugated phalloidin and 10 μg mL^{-1} of DAPI for 30 min and 5 min, respectively. Subsequently, the cells were visualized using CLSM.

2.7 Fabrication of nerve conduits

The schematic of the fabrication of nerve conduits is illustrated in Fig. 1(g). Briefly, 1.2 g of P(LLA-CL) was dissolved in 10 mL of HFIP to generate 12% w/v P(LLA-CL) solution, which was subsequently applied in single spinneret electrospinning. The applied voltage, electrospinning distance and flow rate were set at 12 kV, 15 cm, and 1.5 mL h^{-1}, respectively. The as-prepared PLLA nanofiber yarns (red in Fig. 1(g), effective length of 6 cm) were parallelly fixed around the metal stick (grey in Fig. 1(g), diameter of 2.5 mm) along the axis of the stick. The stick was fixed on a motor with a rotating rate of 5 rpm and ground to collect the electrospun P(LLA-CL) nanofiber (green in Fig. 1(g)). The electrospinning lasted for two hours. Finally, the metal stick was removed and the conduit was well prepared. The nerve conduit was incubated in a vacuum oven for 48 h to remove the residual solvent.

2.8 *In vitro* cell culture

To test the biocompatibility of the nerve conduit, the as-prepared conduit was cut into short sections with a length of 9 mm. SCs were co-cultured with the conduit sections. The ethanol steam sterilized conduit section was placed in wells of the 24-well plate. After washing with PBS and culture medium, 500 μL of cell solution of 4×10^5 cells per mL was pipetted into the end of each section of the nerve conduit. Afterwards, the conduit sections were kept in the culture plate and incubated on a shaker (60 rpm) in the incubator. The culture medium was refreshed every other day. After 1, 3, and 7 days of culture, the conduit section combined with cells was transferred into a new plate. MTT assay was conducted as described above to determine the amount of viable cells in the conduit.

2.9 Cell proliferation and migration in the nerve conduit

To observe the distribution of cells in the conduit, conduits combined with SCs were fixed after 7 days of culture with 4% paraformaldehyde for 2 h at 4 °C. The samples were embedded in sample freezing medium and plunge frozen at −80 °C. The frozen samples were sliced into thin slices with a thickness of 30 μm at −40 °C. Cross-sections in the axial direction were obtained. Slices were collected on glass slides and stained with DAPI, followed by observed using CLSM.

2.10 Statistical analysis

All the data were obtained at least in triplicate and all values were presented as the mean and standard deviation (SD). Statistical analysis was performed by the one-way analysis of variance using Origin 8.0 (OriginLab Inc., USA). The statistical difference between two sets of data was considered when $*p < 0.05$ and $**p < 0.01$.

3. Results and discussion

3.1 Electrospun nanofiber yarn

Dual spinner electrospinning was conducted to fabricate the PLLA nanofiber yarn with a highly aligned nanofiber. The schematic of yarn fabrication is illustrated in Fig. 1(f) and the SEM images of the nanofiber yarn are shown in Fig. 2. It can be seen that PLLA nanofibers in the surface of the nanofiber yarn were unidirectionally oriented along the axis of the yarn body within a tiny twisting angle α ($8.37 \pm 1.69^\circ$, Fig. 2(a) and (b)). Ali Usman *et al.* reported that increasing the rotating speed of the metal funnel could rise the twisting angle and meanwhile strengthen the mechanical properties.[36] Herein, we chose a low funnel rotating speed of 300 rpm to minimize the twisting angle and got nanofibers aligned to the axis of the yarn. The cross-section of the nanofiber yarn is illustrated in Fig. 2(c). Two or three fibers combined into a bundle with grooves forming between adjacent fibers. Porosity could still be observed in the yarn, which could increase the specific surface area and thus facilitate the transport of nutrition and degradation. The average diameter of the PLLA nanofibers in the yarn was 598.2 ± 215.1 nm (Fig. 2(d)). The average diameter of the PLLA yarn was 49.7 ± 14.6 μm.

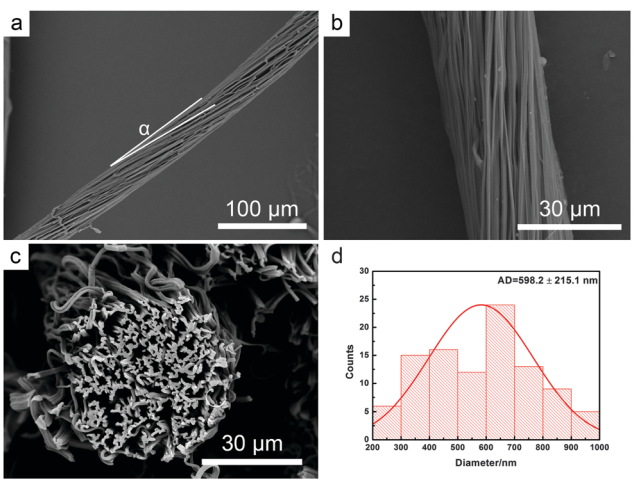

Fig. 2 SEM images of the nanofiber yarn. Morphology of the surface of the PLLA nanofiber yarn (a) and (b). Cross-section of the nanofiber yarn (c). Diameter distribution of the PLLA nanofiber in the nanofiber yarn (d).

3.2 SC adhesion and proliferation

Cell adhesion on the PLLA nanofiber yarn and film was assessed by determining the amount of viable SCs attached to each scaffold using MTT assay. According to our previous research, most SCs could attach to scaffolds in about 4 hours. Thus the time period for cell adhesion was set as 240 min. As illustrated in Fig. 3(a), cells attached to the PLLA nanofiber film kept the least in 240 min culture period. After 240 min of incubation, SCs on the nanofiber yarn are significantly more than that of TCP. MTT analysis shows that the nanofiber yarn had better cell adhesion capacity than nanofiber film, which might further benefit the spreading and proliferation of cells on the scaffold. It is believed that the nanoscale topology and high specific surface area of the nanofiber could mimic the natural extracellular matrix (ECM) and facilitate cell growth and tissue regeneration. However, nanofibrous structure also reduces the pore size of the scaffold, inhibiting cells on the very surface and hindering cell migration into the scaffold. The nanofiber yarn can provide the fluctuant surface of the microscope, which increases the effective surface for cell adherence. Thus, more cells can attach to the scaffold in the initial several hours, enhancing the adhesion of SCs.

Longer period culturing was conducted to study the proliferation of SCs on the nanofiber yarn. MTT assay was conducted after 1, 3, and 7 days of culture to determine the amount of viable cells. As shown in Fig. 3(b), during 7 days of culture, SCs go through a remarkable increase on three groups of substrates, implying that the PLLA nanofiber scaffolds can support the proliferation of SCs. In 3 day post-seeding, more SCs are detected on the PLLA nanofiber yarn than film. The difference is enlarged over time. 7 days later, the amount of SCs on the nanofiber yarn even surpasses that on TCP. It can be obviously concluded that the PLLA nanofiber yarn could significantly enhance SC proliferation. As mentioned above, the microscope structure of the nanofiber yarn can provide more space for cell spreading and migration. As shown in Fig. 4(f), SCs cover the whole surface of the yarn, including the upper side, lateral sides, and even the underside. However, restricted by the small pores between the nanofibers, the film possesses no extra space for cell growth except the upper surface. In addition, the micro-structure of the yarn also facilitates the transport of nutrition and metabolic waste, which also contributes to the cell proliferation.

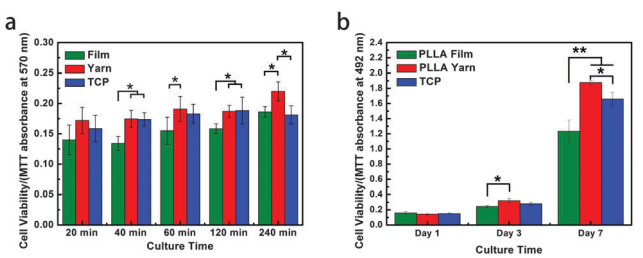

Fig. 3 Analysis of MTT assay for SC adhesion (a) and proliferation (b) on PLLA film, the PLLA nanofiber yarn and TCP. * indicates statistical difference for $p < 0.05$; ** indicates statistical difference for $p < 0.01$.

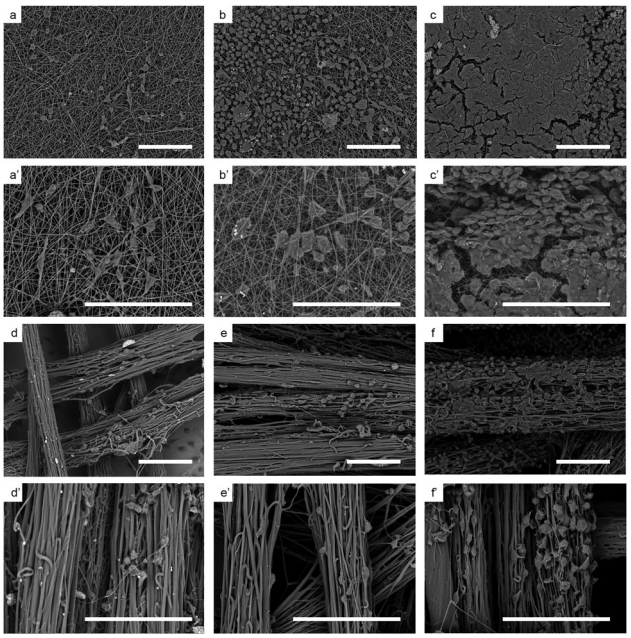

Fig. 4 SEM images of SCs on PLLA film and the PLLA nanofiber yarn after being cultured on PLLA film for 1 day (a and a′), 3 days (b, and b′), 7 days (c and c′), and the PLLA nanofiber yarn for 1 day (d and d′), 3 days (e and e′), and 7 days (f and f′). (x) and (x′) represent different magnifications of 500× and 2000×. (Double sided arrows indicated the yarn axis. Scale bar: 100 μm.)

3.3 Cell morphology

The structure of scaffolds is the key issue for cell colonization in tissue engineering. To study the interaction between cells and different scaffolds, the morphology of SCs on the PLLA nanofiber yarn and film was observed *via* SEM and CLSM images after 1, 3, and 7 days of culture. Fig. 4 and 5 illustrate the SEM images and confocal microscopy of SCs, respectively. For the confocal observation, the SCs were visualized by staining the F-actin and nuclei into red and blue, respectively.

After 1 day of culture, polarized SCs are observed on the nanofiber yarn with the long axis oriented in the direction of the yarn (Fig. 4(d) and (d′)), while on the film, randomly oriented cells of spindle or polygonal shapes are observed (Fig. 4(a) and (a′)).This phenomenon can be confirmed by the confocal images in Fig. 5(a), (a′), (d) and (d′). Longer axons of SCs can be clearly observed along the nanofiber yarn (Fig. 5(d)). These two different phenotypes of SCs evidently observed on two scaffolds become more obviously different in the later culturing period. After 3 days, more cells can be found on both scaffolds (Fig. 4(b) and (e) and 5(b) and (e)). Part of SCs cultured on the film become spread-out, while the rest of the cells are still randomly aligned across multiple fibers and elongated along the fiber axes (Fig. 4(b′) and 5(b′)). In contrast, more SCs with long axons stretched along the nanofiber yarn are observed (Fig. 4(e) and (e′) and 5(e) and (e′)). The parallel red filaments indicate that the aligned nanofiber induces cells extending undirectionally. 7 days after cell seeding, rounded shaped SCs form a densely compacted layer and occupied the whole surface of the film with no evident axons observed (Fig. 4(c) and (c′) and 5(c) and (c′)).

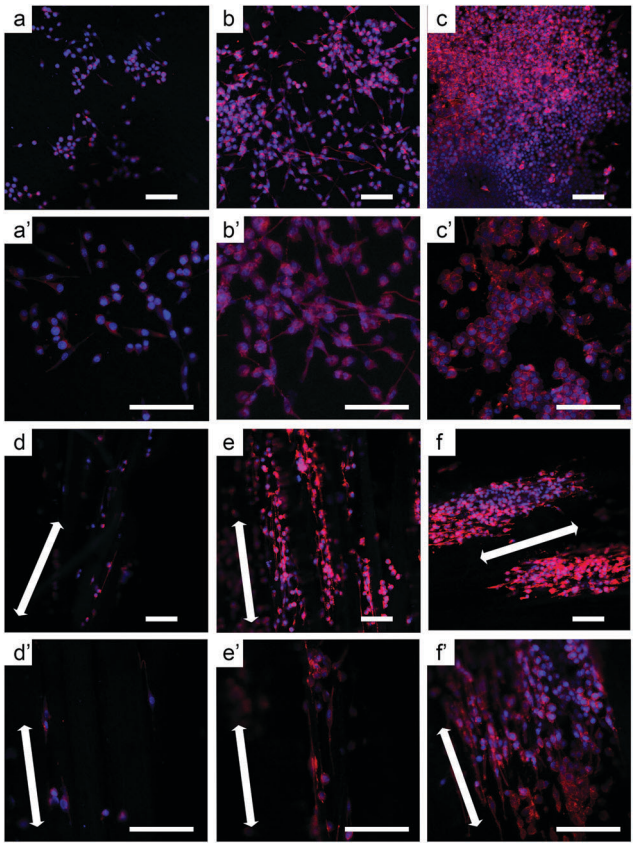

Fig. 5 CLSM microscopy images of SCs on PLLA film and the PLLA nanofiber yarn after being cultured on PLLA film for 1 day (a and a′), 3 days (b and b′), and 7 days (c and c′), and the PLLA nanofiber yarn for 1 day (d and d′), 3 days (e and e′), and 7 days (f and f′). (x) and (x′) represent different magnifications of 500× and 2000×. (Double sided arrows indicated the yarn axis. Scale bar: 100 μm.)

However, the trend on the nanofiber yarn remains unchanged as the number of SCs expands over time. More aligned SCs surround the nanofiber yarn with only part of the surface taken up, leaving sufficient space for further cell migration and proliferation.

Previous studies have indicated that parallel nanofibers determined the spreading and migration, as well as the neurite outgrowth of nerve cells.[8,19] However, the crossed fibers inhibited the further axonal extension of SCs, which may be detrimental in the growth of efficient and directed axons. Additionally, aligned fibers also induced the differentiation and maturation of neural stem cells and SCs.[25,37] Highly aligned nanofiber scaffolds possessed the potential in nerve regeneration for the cure of peripheral nerve injuries. Herein, the nanofiber yarn constructed by nanofibers highly aligned along the axis of the yarn was fabricated *via* a dual needle electrospinning system. SCs were cocultured with the yarn as well as film to assess axon outgrowth and SC behavior. SC cultured showed a polarized structure along the axis of the yarn, and the trend did not change over time during the culture period. However, SCs on the film were randomly oriented with a spread-out phenotype. As the time prolonged, SCs occupied the finite surface of the film and transformed into a rounded shape. Without more space for cell spreading, the proliferation of SCs was inhibited and the outgrowth of axons was hindered. In contrast, the microscopic structure constructed by the nanofiber yarn enlarged the effective space for cell migration and proliferation. Moreover, SCs on the nanofiber yarn could colonize in a three-dimensional space, which may be favorable for long time implantation and leave enough time for the regeneration of new nerve tissue *in vivo*.

3.4 Fabrication of nerve conduits with PLLA nanofiber yarns

As manually inserting the nanofiber yarn into a hollow tube may cause additional curves and entanglements of yarns during operation, resulting in a disordered structure in the lumen, the entangled yarn would mislead the spread and migration of cells in the conduit, consuming more time for the enclosure of the nerve defection. To generate a uniform arrangement, the nanofiber yarn constructed by highly aligned nanofibers was incorporated into a nanofibrous conduit of P(LLA-CL) nanofibers as illustrated in Fig. 1(g). PLLA yarns of two hundred are straightened and parallelly adhered around a metal stick as shown in Fig. 6(a). After electrospinning P(LLA-CL) for 2 h, the surface of the yarn is covered with a thin layer of P(LLA-CL) nanofibers (Fig. 6(b)), which can act as a barrier to limit the penetration of interstitial cells into the guide, as well as facilitate necessary suture while applied in clinic. After the removal of the internal metal stick, a novel P(LLA-CL) nerve conduit filled with PLLA nanofiber yarns is obtained. The conduit was immersed into liquid nitrogen and then cut into short sections for further characterization. The radial cross-section of the conduit was observed by SEM and is shown in Fig. 6(c) and (d). It can be

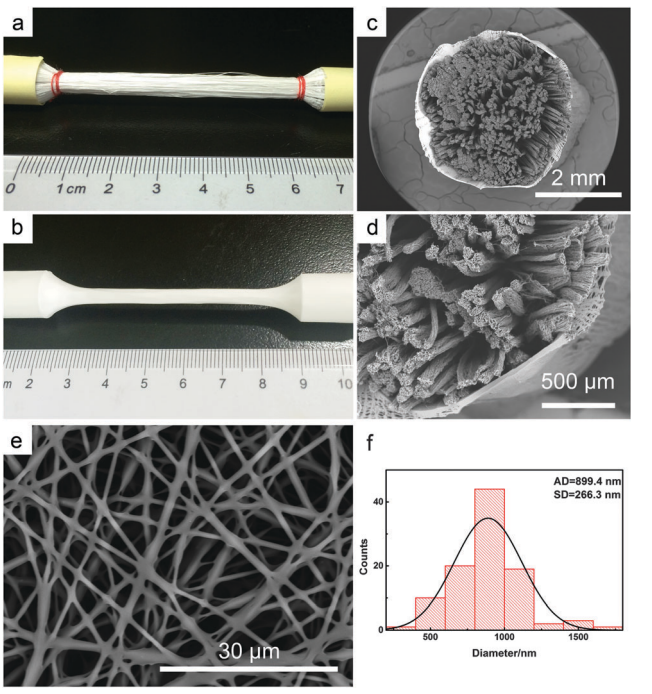

Fig. 6 Photo of the metal stick surrounded by the PLLA nanofiber yarn (a). Photo of the nerve conduit after electrospun P(LLA-CL) (b). SEM images of the cross-section of the nerve conduit 30× (c) and 100× (d). SEM image (e) and diameter distribution (f) of the P(LLA-CL) layer.

seen that the yarns are parallelly inserted in the lumen of the conduit with less curve and entanglement. The inserted yarns can provide proper support and the highly aligned nanofiber in the yarn can generate topological guidance for cell migration and neurite outgrowth across the nerve bridge. The SEM image of the P(LLA-CL) layer is shown in Fig. 6(e). The average diameter of the P(LLA-CL) nanofiber is 899.4 ± 266.3 nm.

In addition, porosity in the lumen of the conduit is a key factor for nerve cell spreading, colonization, proliferation, as well as new nerve tissue in growth. Simply filling conduits with aligned fibers may block the channels and hinder the infiltration and migration of cells.[18,21] For this conduit, the porosity between yarns left enough space for further cell migration. The percentage of the open region was determined by the density of nanofiber yarns. For a given inner diameter of the conduit, the porosity increases while decreasing the number of nanofiber yarns inserted in. Thus the porosity was controllable for a specific demand.

3.5 SC proliferation and migration in the conduit

SCs were seeded in the nerve conduit sections with a length of 9 mm by pipetting a certain amount of SCs into the lumen from one end of the conduit. The substrates seeded with cells were placed in a shaker. The nutrition and metabolic waste could only be transferred through the P(LLA-CL) wall or the two ends of the conduit. As illustrated in Fig. 7, the MTT assay indicates that the amount of SCs in the conduits go through a slight increase during the 7 days of culture, indicating the good biocompatibility of the nerve conduit. Obviously, the increasing rate is much slower compared with those cultured on the PLLA nanofiber yarn (Fig. 3(b)). This can be attributed to the methods of viability determination. Part of the formazan form during MTT incubation may not be dissolved by DMSO owing to the barrier of the P(LLA-CL) wall, resulting in a relatively lower absorbance.

Fig. 8 illustrates the morphology of SCs growing in the conduit. The cultivated SCs show no visible difference in appearance compared with those cultured on the nanofiber yarn. On a single yarn,

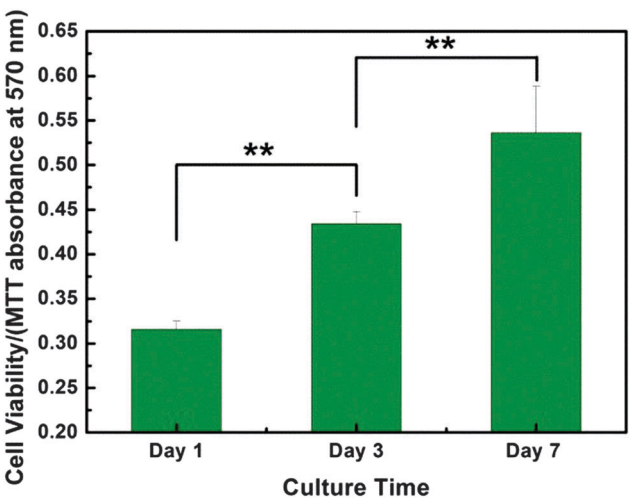

Fig. 7 MTT assay of SCs cultured in the nerve conduit.

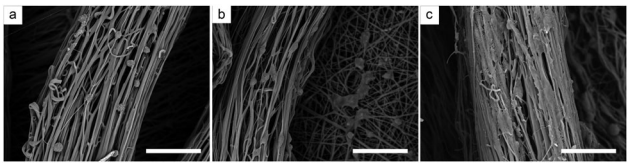

Fig. 8 SEM images of SCs cultured in the conduit sections for 1 (a), 3 (b), and 7 days (c). (Scale bar: 50 μm.)

the amount of SCs increases over culturing time. On the conduit wall of P(LLA-CL), randomly oriented SCs are observed in Fig. 8(b).

To determine the distribution of the SCs in the conduit, cells were labeled by DAPI to generate blue fluorescence and visualized by CLSM. Fig. 9 demonstrates the confocal microscopy photos of the longitudinal section of the nerve conduit combined with SCs after 7 days of culture. SCs can be observed from the wall (Fig. 9(a)) to the center of the conduit lumen (Fig. 9(a)). Moreover, across the longitudinal axis of the conduit, the amount of SCs shows little difference, indicating that SCs had migrated through the entire lumen. According to the SEM images shown in Fig. 8(c), after 7 days of culture, SCs have already covered most surface of the nanofiber yarn, which made it evident that the filling nanofiber yarn can positively promote the spreading and migration of SCs in the conduit.

Topological cues could significantly affect the behavior of SCs including elongation, migration, alignment, as well as subsequent axon extension. A previous study indicated that the size scale matters in the alignment and outgrowth of axons, which became significantly improved while the fiber diameter was lowered down from hundreds of micrometer to hundreds of nanometer.[38,39] The electrospun fiber with a diameter ranging from tens of nanometer to several micrometers has drawn considerable attention in the fabrication of nerve tissue engineering scaffolds. Herein, the PLLA nanofiber yarn with highly aligned nanofibers was fabricated *via* a dual spinneret electrospinning system. Parallel nanofibers twisted into a bundle maintained the guidance cues as the 2D film in addition to microscale structure and feasibility for further processing. *In vitro* experiments demonstrated that the PLLA nanofiber yarn scaffold could promote SC proliferation due to its 3D structure and high effective surface. The proliferating SCs could express various ECM cell adhesion molecules and plentiful growth promoting factors, enhancing the further outgrowth of axons.[40] The unidirectional nanofiber in the surface also accelerated the elongation and orientation of SCs and increased the length of axons.

After the injury of the peripheral nerve, SCs proliferate, reorganize, and align to form bands of Bungner.[19] A nerve conduit is needed to bridge the lesion, providing a guiding framework for the proliferation of neurons and promoting the related cells to generate inductive factors for axon outgrowth. Nanofiber filaments, bundles, or 3D scaffolds with parallel nanofibers were inserted into hollow tubes for enhanced cell alignment and migration. However, the manual operation is always performed in entanglement of nanofibers and collapse of the parallel structure, which would impede the growth of the regenerated nerve. Moreover, the structure of the filaments, bundles,

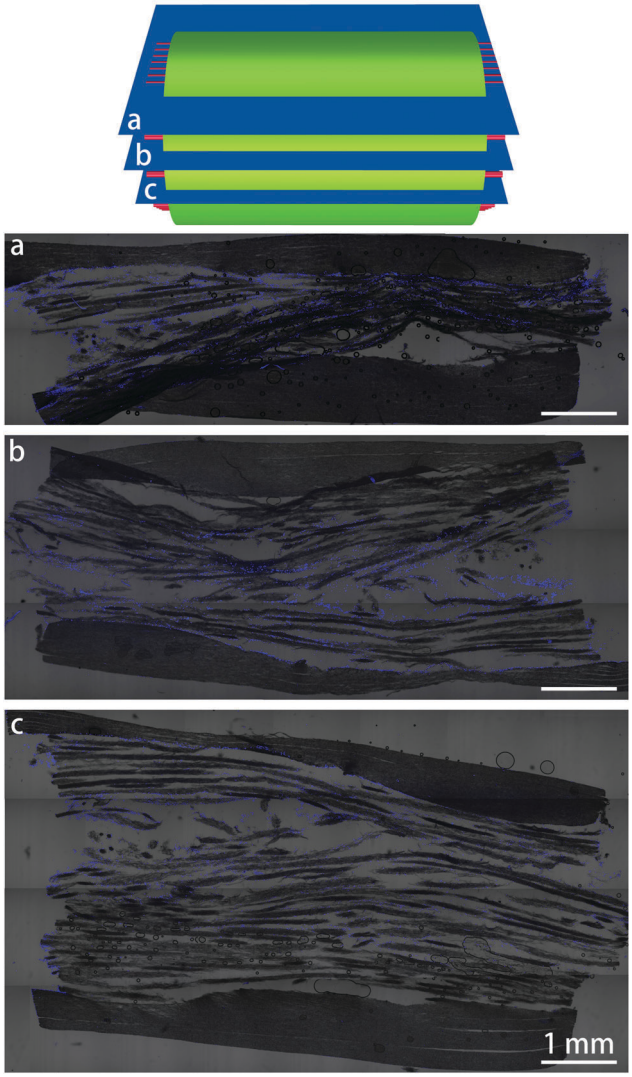

Fig. 9 Longitudinal cross-section of the nerve conduit after coculturing with SCs for 7 days. (a–c) presented different levels of the conduit shown in the schematic diagram.

and 3D nanofibers was quite hard to qualitatively control. In this study, we incorporated the uniform PLLA nanofiber yarn consists of longitudinally aligned nanofibers into a P(LLA-CL) tube to fabricate a novel nerve conduit for peripheral nerve regeneration. The PLLA nanofiber yarn distributed in a 3D configuration in the conduit provides support for cell adhesion and migration through the entire lumen, while the aligned PLLA nanofiber guided the SC growth in a predetermined direction. In addition, the structure of the conduit including the conduit diameter and the open area could be adjusted to realize a specific design for clinical demands.

In the present study, a synthetic PLLA nanofiber yarn could enhance the alignment, elongation of SCs and outgrowth of axons. However, for further research, *in vivo* experiment needs to be conducted to assess the actual function of this novel conduit in nerve regeneration. Natural materials of better biocompatibility or the combination of natural and synthetic materials could also be employed to construct the aligned yarn and conduit. Thus, quite a number of materials and their combination could be fabricated into a nanofiber yarn to study the ability in generating a new nerve. Moreover, a surface modified or drug loaded nanofiber might be processed using the same method to obtain better results in the repair of peripheral nerve injuries.

4. Conclusion

In peripheral nerve injuries, nerve conduit bridges between the broken stumps provide proper configuration to facilitate support cell distribution and the growth of injured nerve tissues in a predetermined direction. Herein, a novel conduit was fabricated with the PLLA nanofiber yarn as the inner filler and the P(LLA-CL) nanofiber layer as the surrounding shell. *In vitro* experiments indicated the good biocompatibility and guiding capacity for spreading, migration, and alignment of SCs. SCs cultured in the conduit section migrated through the entire space in the conduit. Based on the present data, it was believed that the conduit possessed the ability for peripheral nerve repair, which would be experimentally evaluated in further studies.

Acknowledgements

This research was supported by National Natural Science Foundation of China (31470941, 31271035, and 51403033), Science and Technology Commission of Shanghai Municipality Program (14JC1492100, 15441905100), PhD Programs Foundation of Ministry of Education of China (20130075110005) and light of textile project (J201404), the Fundamental Research Funds for the Central Universities (CUSF-DH-D-2014011and 2232014D3-15), and the Deanship of Scientific Research at King Saud University for its funding of this research through the research group project no. RGP-201.

References

1 C. E. Schmidt and J. B. Leach, *Annu. Rev. Biomed. Eng.*, 2003, **5**, 293–347.
2 J. H. Bell and J. W. Haycock, *Tissue Eng., Part B*, 2012, **18**, 116–128.
3 J. Li, T. A. Rickett and R. Shi, *Langmuir*, 2008, **25**, 1813–1817.
4 L. Yao, G. C. de Ruiter, H. Wang, A. M. Knight, R. J. Spinner, M. J. Yaszemski, A. J. Windebank and A. Pandit, *Biomaterials*, 2010, **31**, 5789–5797.
5 F. Gelain, L. D. Unsworth and S. Zhang, *J. Controlled Release*, 2010, **145**, 231–239.
6 J. Xie, M. R. MacEwan, A. G. Schwartz and Y. Xia, *Nanoscale*, 2010, **2**, 35–44.
7 A. S. Hanna and R. Dempsey, *Neurosurgery*, 2010, **67**, N14–N15.
8 H. B. Wang, M. E. Mullins, J. M. Cregg, C. W. McCarthy and R. J. Gilbert, *Acta Biomater.*, 2010, **6**, 2970–2978.
9 T. Nakamura, Y. Inada, S. Fukuda, M. Yoshitani, A. Nakada, S. Itoi, S. Kanemaru, K. Endo and Y. Shimizu, *Brain Res.*, 2004, **1027**, 18–29.

10 D. Ceballos, X. Navarro, N. Dubey, G. Wendelschafer-Crabb, W. R. Kennedy and R. T. Tranquillo, *Exp. Neurol.*, 1999, **158**, 290–300.

11 T. Toba, T. Nakamura, Y. Shimizu, K. Matsumoto, K. Ohnishi, S. Fukuda, M. Yoshitani, H. Ueda, Y. Hori and K. Endo, *J. Biomed. Mater. Res.*, 2001, **58**, 622–630.

12 F. Stang, H. Fansa, G. Wolf, M. Reppin and G. Keilhoff, *Biomaterials*, 2005, **26**, 3083–3091.

13 S. Yoshii, S. Ito, M. Shima, A. Taniguchi and M. Akagi, *J. Tissue Eng. Regener. Med.*, 2009, **3**, 19–25.

14 H. S. Koh, T. Yong, W. E. Teo, C. K. Chan, M. E. Puhaindran, T. C. Tan, A. Lim, B. H. Lim and S. Ramakrishna, *J. Neural Eng.*, 2010, **7**, 046003.

15 B. S. Jha, R. J. Colello, J. R. Bowman, S. A. Sell, K. D. Lee, J. W. Bigbee, G. L. Bowlin, W. N. Chow, B. E. Mathern and D. G. Simpson, *Acta Biomater.*, 2011, **7**, 203–215.

16 M. F. Daud, K. C. Pawar, F. Claeyssens, A. J. Ryan and J. W. Haycock, *Biomaterials*, 2012, **33**, 5901–5913.

17 J. Cao, C. Sun, H. Zhao, Z. Xiao, B. Chen, J. Gao, T. Zheng, W. Wu, S. Wu, J. Wang and J. Dai, *Biomaterials*, 2011, **32**, 3939–3948.

18 E. M. Jeffries and Y. Wang, *Biofabrication*, 2013, **5**, 035015.

19 Y. T. Kim, V. K. Haftel, S. Kumar and R. V. Bellamkonda, *Biomaterials*, 2008, **29**, 3117–3127.

20 C. Hinuber, K. Chwalek, F. J. Pan-Montojo, M. Nitschke, R. Vogel, H. Brunig, G. Heinrich and C. Werner, *Acta Biomater.*, 2014, **10**, 2086–2095.

21 A. Kriebel, M. Rumman, M. Scheld, D. Hodde, G. Brook and J. Mey, *J. Biomed. Mater. Res., Part B*, 2014, **102**, 356–365.

22 P. Sangsanoh, S. Waleetorncheepsawat, O. Suwantong, P. Wutticharoenmongkol, O. Weeranantanapan, B. Chuenjitbuntaworn, P. Cheepsunthorn, P. Pavasant and P. Supaphol, *Biomacromolecules*, 2007, **8**, 1587–1594.

23 J. Xie, M. R. MacEwan, W. Liu, N. Jesuraj, X. Li, D. Hunter and Y. Xia, *ACS Appl. Mater. Interfaces*, 2014, **6**, 9472–9480.

24 C. Huang, Y. Tang, X. Liu, A. Sutti, Q. Ke, X. Mo, X. Wang, Y. Morsi and T. Lin, *Soft Matter*, 2011, **7**, 10812.

25 S. Y. Chew, R. Mi, A. Hoke and K. W. Leong, *Biomaterials*, 2008, **29**, 653–661.

26 W. Martens, K. Sanen, M. Georgiou, T. Struys, A. Bronckaers, M. Ameloot, J. Phillips and I. Lambrichts, *FASEB J.*, 2014, **28**, 1634–1643.

27 X. Gu, F. Ding, Y. Yang and J. Liu, *Prog. Neurobiol.*, 2011, **93**, 204–230.

28 Y. Zhu, A. Wang, W. Shen, S. Patel, R. Zhang, W. Young and S. Li, *Adv. Funct. Mater.*, 2010, **20**, 1433–1440.

29 S. Y. Chew, R. Mi, A. Hoke and K. W. Leong, *Adv. Funct. Mater.*, 2007, **17**, 1288–1296.

30 F. Ko, Y. Gogotsi, A. Ali, N. Naguib, H. Ye, G. L. Yang, C. Li and P. Willis, *Adv. Mater.*, 2003, **15**, 1161–1165.

31 E. Smit, U. Bűttner and R. D. Sanderson, *Polymer*, 2005, **46**, 2419–2423.

32 W.-E. Teo, R. Gopal, R. Ramaseshan, K. Fujihara and S. Ramakrishna, *Polymer*, 2007, **48**, 3400–3405.

33 X. Wang, K. Zhang, M. Zhu, H. Yu, Z. Zhou, Y. Chen and B. S. Hsiao, *Polymer*, 2008, **49**, 2755–2761.

34 M. S. M. Jad, S. A. H. Ravandi, H. Tavanai and R. H. Sanatgar, *Fibers Polym.*, 2011, **12**, 801–807.

35 H. Yan, L. Liu and Z. Zhang, *Mater. Lett.*, 2011, **65**, 2419–2421.

36 U. Ali, Y. Zhou, X. Wang and T. Lin, *J. Text. Inst.*, 2012, **103**, 80–88.

37 L. He, S. Liao, D. Quan, K. Ma, C. Chan, S. Ramakrishna and J. Lu, *Acta Biomater.*, 2010, **6**, 2960–2969.

38 X. Wen and P. A. Tresco, *J. Biomed. Mater. Res., Part A*, 2006, **76**, 626–637.

39 F. Yang, R. Murugan, S. Wang and S. Ramakrishna, *Biomaterials*, 2005, **26**, 2603–2610.

40 S. Madduri, M. Papaloizos and B. Gander, *Biomaterials*, 2010, **31**, 2323–2334.